Cell Death and Differentiation (2007), 1–4

www.nature.com/cdd

Letter to the Editor

The proapoptotic BCL-2 family member BIM mediates motoneuron loss in a model of amyotrophic lateral sclerosis

Cell Death and Differentiation advance online publication, 18 May 2007; doi:10.1038/sj.cdd.4402166

Dear Editor,

Amyotrophic lateral sclerosis (ALS) is a progressive adult-onset motoneuron disease characterized by muscle weakness, atrophy, paralysis and premature death. The pathological hallmark of ALS is the selective degeneration of motoneurons in the spinal ventral horn, most brainstem nuclei and cerebral cortex.[1] The majority of ALS patients lack a defined hereditary genetic component and are considered sporadic, whereas approximately 10% of cases are familial (FALS). Over 100 mutations in the gene encoding superoxide dismutase-1 (SOD1), which trigger the misfolding and abnormal aggregation of SOD1, have been genetically linked with FALS.[1] Overexpression of human FALS-linked SOD1 mutations in transgenic mice provokes age-dependent protein aggregation, paralysis and motoneuron degeneration suggesting a direct involvement of misfolded SOD1 in the disease process.[1] The primary mechanism by which mutations in SOD1 contribute to progressive motoneuron loss in FALS remains unknown. It has been proposed that motoneuron apoptosis is mediated by different mechanisms including mitochondrial dysfunction, altered axonal transport, endoplasmic reticulum stress and other non-neuronal components (reviewed by Pasinelli and Brown[1]).

The BCL-2 family of proteins is a group of evolutionarily conserved regulators of cell death that operate at the mitochondrial membrane to control caspase activation. The BCL-2 family is comprised of pro- and antiapoptotic members, and is defined by the presence of up to four conserved domains within their primary structure.[2] Antiapoptotic BCL-2 family members display sequence homology in four α-helical domains called BCL-2 homology (BH)1 to BH4 (i.e. BCL-2 and BCL-X_L). Proapoptotic members can be further subdivided into more fully conserved, 'multidomain' members containing BH1-3 (i.e. BAX and BAK) or the 'BH3-only'members (i.e. BID, BIM, PUMA and BAD) that contain a single α-helical domain critical for activation of apoptosis. Multidomain BAX and BAK function in concert as an essential gateway to the intrinsic cell death pathways operating at the mitochondria, constituting the main core proapoptotic pathway.[2] The upstream BH3-only members respond to particular apoptotic signals and subsequently trigger the conformational activation of BAX and BAK, inducing their intramembranous homo-oligomerization and resultant permeabilization of the mitochondrial outer membrane.[2] Released mitochondrial proteins, such as cytochrome *c*, trigger the activation of caspases through the apoptosome complex.

Alterations in the expression of different BCL-2 family members have been described in the spinal cord of transgenic mice expressing mutant SOD1 and in humans affected with ALS.[3,4] Moreover, survival of $SOD1^{G93A}$ mice is prolonged by the administration of caspase inhibitors or by the overexpression of BCL-2.[5–7] A direct interaction between BCL-2 and mutant SOD1 has been proposed to occur at mitochondria, which may contribute to FALS pathogenesis.[8] A recent report showed that BAX deletion slightly increases the survival of $SOD1^{G93A}$ mice, but it strongly protects motoneurons against apoptosis.[9] This suggests that, in addition to cell death, loss of neuronal functionality is responsible for motoneuron dysfunction in FALS. Although it is known that BAX mediates motoneuron apoptosis in FALS, the upstream death signals that activate the core proapoptotic pathway remain unidentified.

We therefore chose to investigate the involvement of upstream BH3-only proteins in FALS, as these proteins are good candidates as Bax modulators. We first determined the expression levels of different BCL-2 family members in the spinal cord of $hSOD1^{G93A}$ and $mSOD1^{G86R}$ transgenic mice including several BH3-only proteins (BIM, BMF, BAD, PUMA, NOXA, BID and BIK), the proapoptotic BAX and BAX, and the antiapoptotic BCL-X_L and BCL-2 proteins (Supplementary Figure S1). Using quantitative RT-PCR, we observed an increase in the mRNA levels of the proapoptotic BH3-only member *bim* in the spinal cord of post-symptomatic $SOD1^{G85R}$ transgenic mice, when paralysis of the hind legs was observed (Supplementary Figure S1), whereas only a slight increase in the mRNA levels of the BH3-only proteins *bid* and *noxa* were detected in the same samples. No significant changes were observed in the mRNA levels of *bad*, *bmf*, *bik*, *puma*, *bax and bak*. In contrast, an increase in the mRNA levels of *bcl-2* and *bcl-xL* mRNA was observed. Consistent with the mRNA induction of *bim*, Western blot analysis of spinal cord extracts revealed that the BIM extra long (BIM_{EL}) is induced at the protein level in the spinal cord of post-symptomatic $SOD1^{G93A}$ and $SOD1^{G86R}$ transgenic mice (Figure 1a). A slight increase in the expression levels of PUMA was observed, whereas the levels of other proapoptotic proteins, such as BAX, BID or BAK, were not significantly altered (Figure 1a and Supplementary 2S1). In addition, an upregulation of antiapoptotic BCL-X_L and BCL-2 was observed to different extents in the two mutant SOD1-transgenic mice analyzed (Figure 1a and Supplementary S2a). These

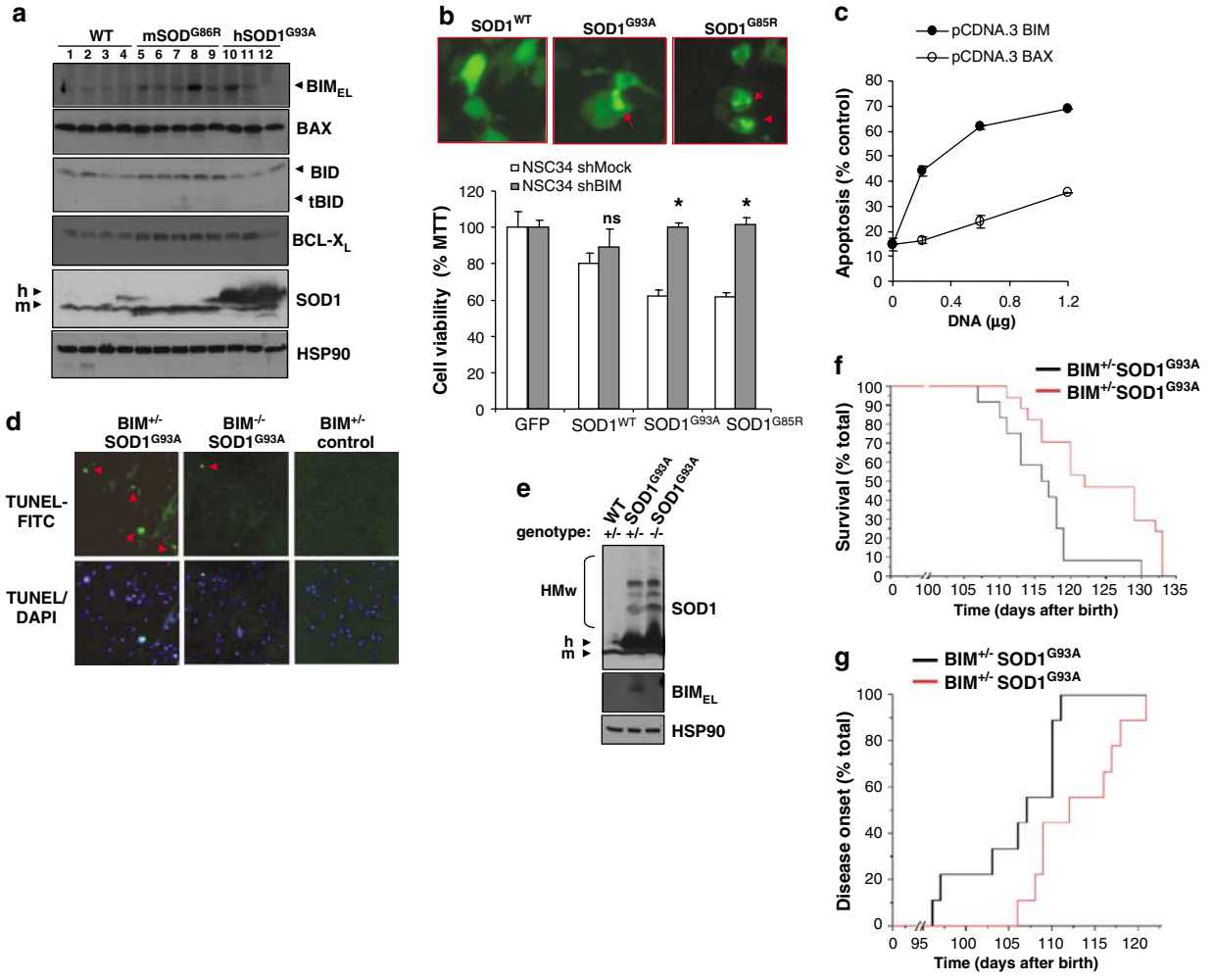

Figure 1 Upregulation of the pro-apoptotic protein BIM mediates motoneuron loss in cellular and mouse ALS models. (**a**) The expression levels of BIM, BAX, BID, BCL-X_L, and SOD1 were analyzed in spinal cord extracts from different symptomatic $SOD1^{G93A}$, $SOD1^{G86R}$ or control mice by Western blot. Animals are between 115 to 125 days of age. Line 12 represents a *bim* deficient mouse. As loading controls, the expression levels of Hsp90 are shown. (**b**) NSC34 cells were stably transduced with lentiviral vectors expressing shRNA against the *bim* or *luciferase* mRNA (Mock), and cell viability was quantified 72 h after transfecting expression vectors for $SOD1^{WT}$, $SOD1^{G93A}$ or $SOD1^{G86R}$–EFGP fusion proteins using the MTS viability assay. Experiments were performed in the presence of 0.5% serum. As control, cells were transfected with an EGFP expression vector and this is considered as 100% viability. Upper panel: The generation of SOD1-EGFP aggregates was visualized by fluorescent microscopy. Asterisks represent *P*-values < 0.001 obtained using Student's t test of comparing Mock versus shRNA for BIM (ns, not significantly different). (**c**) NSC34 cells were transiently transfected with indicated amounts of expression vectors for BIM or BAX, and the percentage of apoptosis was quantified after 24 h by FACS using Annexin-V-PE staining. (**d**) The number of TUNEL-FITC positive cells (apoptotic cells) was visualized in the spinal cord of BIM deficient mice or BIM heterozygous mice carrying a human SOD^{G93A} allele. Animals shown represent littermate controls of the same age (120 days). Results are representative of the analysis of three different mice per group. (**e**) The levels of $hSOD1^{G93A}$ aggregation and BIM were determined by Western blot in BIM deficient and BIM heterozygous mice. As negative control non transgenic BIM heterozygous mice are shown. Of note, high molecular weight (HMw) SOD1 aggregates are observed in the analysis. As controls the expression levels of BIM and Hsp90 are shown. (**f**) Kaplan–Meier survival curves of BIM deficient ($N = 15$) or BIM heterozygous ($N = 17$) mice bearing a $hSOD1^{G93A}$ allele. (**g**) The disease onset of BIM deficient ($N = 15$) or BIM heterozygous ($N = 17$) mice bearing a $hSOD1^{G93A}$ allele was determined and plotted against time. Disease onset was defined as the appearance of abnormal limb-clasping, slight tremor felt in one of the hind-limbs, wobbly gait and the first signs of paralysis in one hind-limb

results contrast with previous findings in which BCL-2 and BCL-X_L levels were decreased in the model, possibly owing to analysis at different stages of the disease or variability in mouse genetic background.[3]

BIM is a potent activator of apoptosis and, in neurons, induces the direct activation of BAX.[10] BIM upregulation is involved in neuronal loss induced by growth factor deprivation and brain seizures, and it is a critical mediator of ischemia-brain injury.[10–12] The function of BIM in neuronal death may not represent a general pro-death activity, as BIM deficiency does not protect mutant *Lurcher* mice from neurodegeneration.[13] In order to establish the role of BIM in the toxicity of SOD1 mutants, we targeted *bim* mRNA with small hairpin RNA (shRNA) using lentiviral-based delivery in the motoneuron cell line NSC34 (Supplementary Figure S2b). Overexpression of $SOD1^{G93A}$- or $SOD1^{G86R}$–EGFP fusion proteins leads to the aggregation of SOD1 in NSC34 cells (Figure 1b and Supplementary Figure S2c) as described previously.[14] Knockdown of BIM completely protected NSC34 cells from mutant SOD1 toxicity after transient transfection (Figure 1b),

suggesting that BIM is part of the proapoptotic pathway triggered by SOD1 aggregates. In agreement with this hypothesis, transient expression of BIM_{EL} induced high levels of apoptosis when compared with BAX, indicating that motoneurons are highly susceptible to changes in BIM expression (Figure 1c).

In order to evaluate the role of BIM in FALS *in vivo*, we generated a BIM-deficient mouse and crossed it with a transgenic mouse overexpressing human $SOD1^{G93A}$. Deletion of BIM drastically decreased the number of TUNEL-positive cells in the ventral horn of $SOD1^{G93A}$ mice (Figure 1d), similar to the effects described by manipulating the levels of BCL-2 or BAX via BCL-2 overexpression or BAX deletion.[5,9] These results suggest that the induction of BIM is upstream of BAX-mediated apoptosis in FALS. In contrast to BAX-deficient mice,[9] only minor changes were observed in motoneurons populating the ventral horn of BIM-deficient mice when compared with littermate controls (Supplementary Figure S2d). This suggests that developmental apoptosis in the spinal cord is not considerably altered in the absence of BIM. Neither the expression levels of human mutant $SOD1^{G93A}$ nor the generation of high molecular weight SOD1 aggregates were drastically affected by abrogation of BIM expression (Figure 1e). Finally, we assessed the possible effects of BIM deletion on the disease onset and survival of $SOD1^{G93A}$ transgenic mice. As shown in Figure 1f, BIM deficiency extended the lifespan of human $SOD1^{G93A}$ transgenic mice when compared with BIM heterozygous mice. The increased survival of BIM-deficient mice was comparable with the effects described for BAX-deficient or BCL-2-over-expressing mice.[5,9] In addition, disease onset was significantly delayed in BIM-deficient mice, supporting a role for this proapoptotic BH3-only protein in motoneuron death in FALS (Figure 1g).

We have provided evidence supporting a role of the proapoptotic protein BIM in FALS. Quantitative determination of the mRNA levels of different proapoptotic BCL-2 family members indicated that BIM is upregulated in a FALS mouse model during the symptomatic stage. Analysis of the role of BIM *in vitro* demonstrated that its expression is required to trigger cell death induced by SOD1 mutants, and that BIM expression *per se* is highly neurotoxic to the well-characterized motoneuron cell line NSC34.[14] In agreement with these observations, ablation of BIM *in vivo* reduced cellular apoptosis in the ventral horn of a transgenic mouse model of FALS, increasing lifespan. These results are novel, as the upstream signals leading to mitochondrial-dependent apoptosis in FALS are not known.

A recent report characterized the hierarchical organization of the BCL-2 family of proteins.[15] Two classes of BH3-only proteins were defined, where BID, BIM and PUMA are strong activators of BAX- and BAK-dependent apoptosis (killers), whereas other BH3-only proteins, such as BAD and NOXA, modulate the pathway by sequestrating antiapoptotic proteins (sensitizers). We did not observe an activation of BID (associated with caspase-dependent cleavage; tBID) in SOD1 transgenic mice. PUMA expression levels were low and a slight but reproducible increase of its expression was detected in our FALS mouse model, suggesting that BIM may be a specific activator of motoneuron death in FALS. The precise contribution of PUMA to ALS remains to be established. In addition to mRNA upregulation, BH3-only proteins are activated by post-translational modifications. Phosphorylation of BIM by the c-Jun N-terminal kinase (JNK) pathway increases its proapoptotic activity, which is known to trigger neuronal death in models of ischemia-reperfusion.[16] BIM resides in an inactive form by binding to the microtubule-associated dynein motor complex and, when released by phosphorylation, promotes BAX-dependent apoptosis.[17] Activation of JNK has been described in astrocytes in models of FALS[18] and disruption of dynein/dynactin interaction inhibits axonal transport in motoneurons causing progressive motor degeneration. It remains to be determined whether or not post-translational modifications of BIM play a role in motoneuron loss in FALS.

Potential therapeutic benefits of targeting the mitochondrial-apoptosis pathway were suggested when enhanced motoneuron survival and improved neuromuscular function of a FALS model was observed after intraspinal injection of an adeno-associated virus encoding BCL-2.[19] BAX and BCL-2 are components of the core proapoptotic pathway, where many different death signals converge to induce apoptosis. Thus, their targeting may have considerable side effects in the long term (i.e. cancer or autoimmunity) by affecting the physiology of other organs. Therefore, it is crucial to identify specific upstream regulators of BAX/BCL-2 in motoneurons as potential therapeutic targets. Pharmacological inhibition of proapoptotic molecules, such as BAX, prevent neuronal death in models of brain ischemia,[20] suggesting that a similar strategy may be feasible to inhibit the activity of BIM. Alternatively, lentiviral delivery of shRNA against *bim* mRNA may be feasible *in vivo* based on the proven success of the method in FALS models. The discovery of specific molecules contributing to motoneuron dysfunction may represent beneficial targets to treat ALS and other fatal motoneuron disorders.

Acknowledgements. We thank Nika Danial for providing support with animal housing. We thank Dorothy Zhang for performing histological analysis of spinal cord tissue. We thank B Turner and J Atkin (University of Melbourne) for providing us expression vectors for SOD1 mutants, N Cashman (McGill University) for providing NSC34 cells and the Broad Institute for kindly providing us shRNA vectors to target BIM. This work was supported by NIH grants P01 CA92625 and R37 CA50239 (SJK); R01 AI32412 and the V Harold and Leila Y Mathers Charitable Foundation (LHG); and FONDECYT no. 1070444 (CH) and FONDAP grant no. 15010006, and a Post Doctoral Fellowship from the Damon Runyon Cancer Research Foundation (CH). R Brown and P Pasinelli receive support for ALS studies from the N.I.N.D.S. the N.I.A., the Al-Athel ALS Research Foundation, the ALS Association, the ALS Therapy Alliance, the Angel Fund, Project ALS and the Pierre L de Bourgknecht ALS Research Foundation.

C Hetz[1,2,3,], P Thielen[1], J Fisher[3], P Pasinelli[4], RH Brown[4], S Korsmeyer[3,✠] and L Glimcher[1,5,*]*

[1] Department of Immunology and Infectious Diseases, Harvard School of Public Health, Boston, MA, USA;
[2] Department of Cellular and Molecular Biology, Institute of Biomedical Sciences, The FONDAP Center for Molecular Studies of the Cell, University of Chile, Santiago, Chile;
[3] Department of Cancer Immunology and AIDS, Howard Hughes Medical Institute, Dana–Farber Cancer Institute, Harvard Medical School, Boston, MA, USA;
[4] Frances & Joseph Weinberg Unit for ALS Research, Farber Institute for Neurosciences, Thomas Jefferson University, Philedelphia, PA, USA and

[5] Department of Medicine, Harvard Medical School, Boston, MA, USA
* Corresponding authors: LH Glimcher, Department of Immunology and Infectious Diseases, FXB Building, Room 205, 651 Huntington Avenue, Boston, MA 02115, USA.
Tel: +1 617 432 0622; E-mail: lglimche@hsph.harvard.edu; or C Hetz, Department of Immunology and Infectious Diseases, FXB Building, Room 205, 651 Huntington Avenue, Boston, MA 02115, USA.
Institute of Biomedical Sciences, University of Chile, Independencia 1029, Santiago 70086, Chile.
Tel: +1 617 432 0249; E-mails: chetz@hsph.harvard.edu and chetz@med.uchile.cl.
* Deceased

1. Pasinelli P, Brown RH. *Nat Rev Neurosci* 2006; **7**: 710–723.
2. Danial NN, Korsmeyer SJ. *Cell* 2004; **116**: 205–219.
3. Gonzalez de Aguilar JL *et al. Neurobiol Dis* 2000; **7**: 406–415.
4. Boillee S, Vande VC, Cleveland DW. *Neuron* 2006; **52**: 39–59.
5. Kostic V *et al. Science* 1997; **277**: 559–562.
6. Li M *et al. Science* 2000; **288**: 335–339.
7. Vukosavic S *et al. J Neurosci* 2000; **20**: 9119–9125.
8. Pasinelli P *et al. Neuron* 2004; **43**: 19–30.
9. Gould TW *et al. J Neurosci* 2006; **26**: 8774–8786.
10. Okuno S, Saito A, Hayashi T, Chan PH. *J Neurosci* 2004; **24**: 7879–7887.
11. Shinoda S *et al. J Clin Invest* 2004; **113**: 1059–1068.
12. Biswas SC, Greene LA. *J Biol Chem* 2002; **277**: 49511–49516.
13. Bouillet P *et al. J Neurosci Res* 2003; **74**: 777–781.
14. Turner B J *et al. J Neurosci* 2005; **25**: 108–117.
15. Kim H *et al. Nat Cell Biol* 2006; **8**: 1348–1358.
16. Putcha GV *et al. Neuron* 2003; **38**: 899–914.
17. Puthalakath H *et al. Mol Cell* 1999; **3**: 287–296.
18. Veglianese P *et al. Mol Cell Neurosci* 2006; **31**: 218–231.
19. Azzouz M *et al. Hum Mol Genet* 2000; **9**: 803–811.
20. Hetz C *et al. J Biol Chem* 2005; **280**: 42960–42970.

Supplementary Information accompanies the paper on Cell Death and Differentiation website (http://www.nature.com/cdd)

Materials and methods

Animal experimentation

To generate mice completely null for *Bim* we adopted a targeting strategy different than that previously reported by Bouillet, et al. (1). Newly targeted mice in which the first 4 exons of the *Bim* gene are deleted by homologous recombination of ES cells were generated to ensure the lack of any aberrant BIM protein (2). This was especially important as the *Bim*-targeted mice generated by Bouillet, et al. (1) were reported to still express an aberrant BIM protein without a BH3 domain, raising the possibility that this partial protein may have affected the phenotype of these mice.

All animal experiments conformed to National Institutes of Health guidelines and were approved by Harvard School of Public Health Animal Care and Use Committee. To minimize differences caused by strain background, we crossed BIM heterozygotes with SOD1 mice [B6SJL-TgN(SOD1-G93A)1Gur] to generate F1 Male SOD1, BIM heterozygotes. Genotyping was performed with standard primers against mutant SOD1 and BIM (2;3). End stage of the disease was determined as the time at which an animal could no longer right itself within 30 s after being placed on its back. In addition disease onset was defined as the appearance of abnormal limb-clasping, slight tremor felt in one of the hind-limbs, wobbly gait and the first signs of paralysis in one hind-limb.

Immunohistochemistry of spinal cord.

For visualizing motoneurons in the ventral horn, consecutive 40 μm-thick cross sections of paraformaldehyde-fixed, sucrose embedded spinal cord tissue were cut and stained with antibodies against the enzyme choline acetyltransferase (ChAT). For detection of apoptosis in spinal cord tissue, sections were stained with the DeadEnd^{TM} fluorometric TUNEL system (Promega, Madison, WI) using FITC fluorescence to identify apoptotic cells following the recommendations of the manufacturer. Images were acquired with a fluorescent confocal microscope. Total nuclei was stained with DAPI.

Cell culture and detection of cell death.

Mouse motor neuron-like NSC-34 cells were supplied by Dr. Neil Cashman (University of Toronto, Toronto, Ontario, Canada). Cell lines were maintained in DMEM with 10%

(v/v) fetal calf serum and 1% (v/v) penicillin–streptomycin (Invitrogen). Cells were subcultured in 6- or 12-well plates (1-2x10^5 cells per well) and were transfected transiently with different concentrations of plasmids using Effectene reagent (Quiagen). For SOD1-EGFP fusion protein, cells were visualized at 72 hr after transfection with an inverted fluorescence microscope. Apoptosis was determined by FACS analysis of cells stained with Annexin-V PE as previously described (*2*). Alternatively, cell viability was quantified in 96 well plates using 3-(4,5-dimethylthazol-2-yl)-5-3-carboxymethoxy-phenyl)-2-(4-sulfophenyl)-2H-tetrazolium (MTS) and phenazine methosulfate according to the recommendations of the supplier (CellTiter 96 AQueous; Promega, Madison, WI). MTS assay after mutant SOD1 overexpression was performed in the presence of low serum (0.5%FBS). Human BIM_{EL} and BAX cDNA were cloned into pCDNA.3 expression vector. Expression vectors for SOD1 mutant proteins in thepEGFP-N1 (Clontech, Palo Alto, CA) were previously described (4).

Generation of stable knockdown of BIM using shRNA.

The Broad Institute (Boston, USA) has designed shRNA molecules to target the mRNA of more than 20,000 genes (5). The oligonucleotide containing shRNA candidates were cloned into the lentiviral vector pLKO.1**,** which contains a puromycin resistant gene and drives the expression of the shRNA under the U6 promoter. Lentiviral particles were prepared by co-transfecting 293T cells (packaging cells) with the pLKO.1 vector and plasmids encoding the envelop protein VSV-g and the packaging plasmid pΔ8.9 (expressing Gag, Pol, etc) as described (5). After 48h of transfection, the media containing the lentivirus was filtered with a 0.45 μm filter and then NSC34 cells were infected with a 1:10 dilution of this supernatant in the presence of 8 μg/ml polybreen. After 24h of infection cells were selected with puromycin (3 μg/ml) for three to five days and the efficiency of mRNA degradation was determined by RT-PCR.

SDS-PAGE and Western Blot Analysis.

Spinal cord tissue was homogenized by sonication on ice in RIPA buffer (20mM Tris pH 8.0, 150mM NaCl, 0.1% SDS, 0.5% DOC, 0.5% triton X-100) containing a protease inhibitor cocktail (Roche, Basel, Germany), NaF 1 mM, sodium orthovanadate and a

phosphatase inhibitor cocktail (Promega) as previously described (6). Protein concentration was determined by micro-BCA assay (Pierce, Rockford, IL). The equivalent of 30–50μg of total protein was loaded onto 12%, 10% or 4-12% SDS-PAGE minigels (Novex NuPage, Invitrogen Life Technologies) and analyzed by Western blotting. The following antibodies and dilutions were used: anti-BIM 1:1000, anti-SOD1 (Calbiochem), anti-BID 1:500 and anti-Hsp90 1:3000 (Santa Cruz); anti-PUMA 1:1000 (Sigma); anti-BAX and anti-BAK 1:1000 (Upstate Technology); anti-BCL-2 and anti-BCL-X_L 1:1000 (B.D. transduction laboratories). After incubation with the primary antibody overnight at 4°C, membranes were washed and incubated for 1h at room temperature with horseradish peroxidase-coupled second antibodies (Amersham Biosciences) diluted 1:5000 in washing buffer. After washing, specifically bound antibodies were detected by enhanced chemiluminescence assay (Amersham Biosciences).

RNA extraction and quantitative RT-PCR.

Total RNA was prepared from spinal cord tissue or cell lines using trizol (Invitrogen, Carlsbad, CA) and cDNA was synthesized with SuperScript III (Invitrogen, Carlsbad, CA) using random primers $p(dN)_6$ (Roche, Basel, Switzerland). Quantitative real-time PCR reactions employing SYBR green fluorescent reagent were done in an ABI PRISM 7700 system (Applied Biosystems, Foster City, CA). The relative amounts of mRNAs were calculated from the values of comparative threshold cycle by using beta actin as control. Primer sequences were designed by Primer Express software (Applied Biosystems, Foster City, CA). Real time PCR was performed as previously described (7;8) using the primers described in supplementary Table 1.

Reference List

1. Bouillet, P., Metcalf, D., Huang, D. C., Tarlinton, D. M., Kay, T. W., Kontgen, F., Adams, J. M., and Strasser, A. (1999) *Science* **286,** 1735-1738

2. Takeuchi, O., Fisher, J., Suh, H., Harada, H., Malynn, B. A., and Korsmeyer, S. J. (2005) *Proc. Natl. Acad. Sci. U. S. A* **102,** 11272-11277

3. Pasinelli, P., Belford, M. E., Lennon, N., Bacskai, B. J., Hyman, B. T., Trotti, D., and Brown, R. H., Jr. (2004) *Neuron* **43,** 19-30

4. Turner, B. J., Atkin, J. D., Farg, M. A., Zang, d. W., Rembach, A., Lopes, E. C., Patch, J. D., Hill, A. F., and Cheema, S. S. (2005) *J. Neurosci.* **25,** 108-117

5. Moffat, J., Grueneberg, D. A., Yang, X., Kim, S. Y., Kloepfer, A. M., Hinkle, G., Piqani, B., Eisenhaure, T. M., Luo, B., Grenier, J. K., Carpenter, A. E., Foo, S. Y., Stewart, S. A., Stockwell, B. R., Hacohen, N., Hahn, W. C., Lander, E. S., Sabatini, D. M., and Root, D. E. (2006) *Cell* **124,** 1283-1298

6. Hetz, C., Russelakis-Carneiro, M., Maundrell, K., Castilla, J., and Soto, C. (2003) *EMBO J.* **22,** 5435-5445

7. Hetz, C., Bernasconi, P., Fisher, J., Lee, A. H., Bassik, M. C., Antonsson, B., Brandt, G. S., Iwakoshi, N. N., Schinzel, A., Glimcher, L. H., and Korsmeyer, S. J. (2006) *Science* **312,** 572-576

8. Lee, A. H., Chu, G. C., Iwakoshi, N. N., and Glimcher, L. H. (2005) *EMBO J.* **24,** 4368-4380

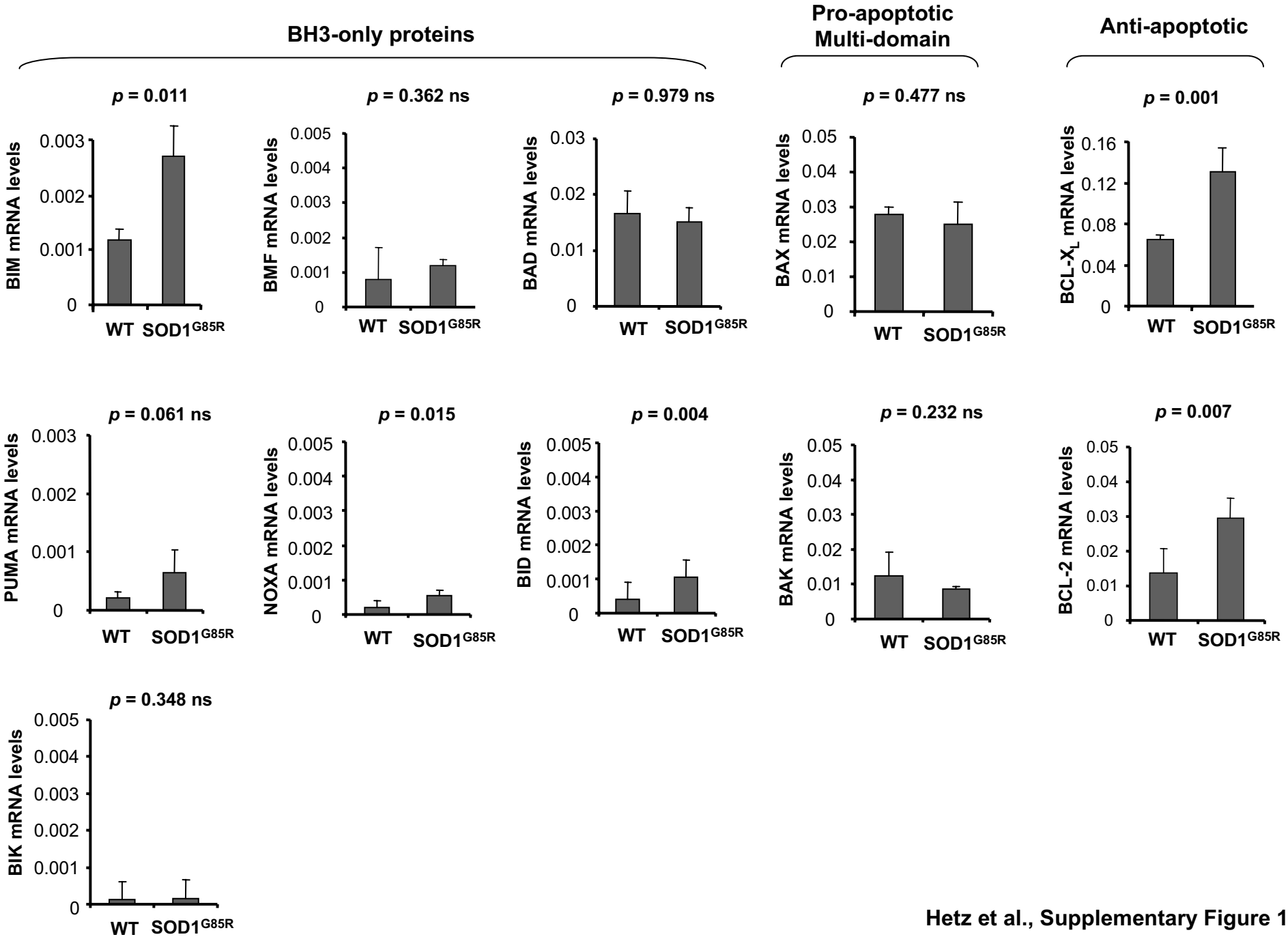

Hetz et al., Supplementary Figure 1

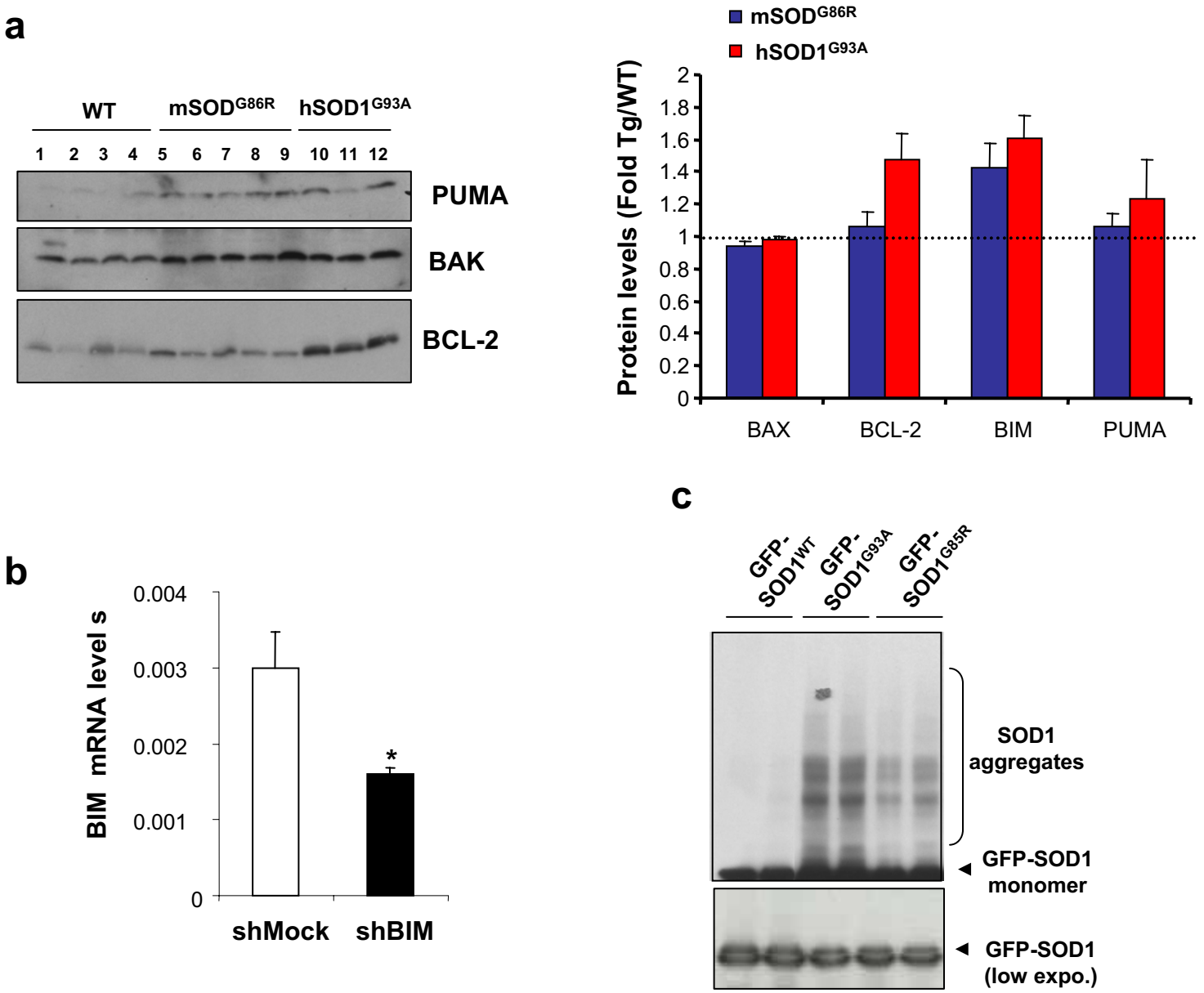

Hetz et al., Supplementary Figure 2

d

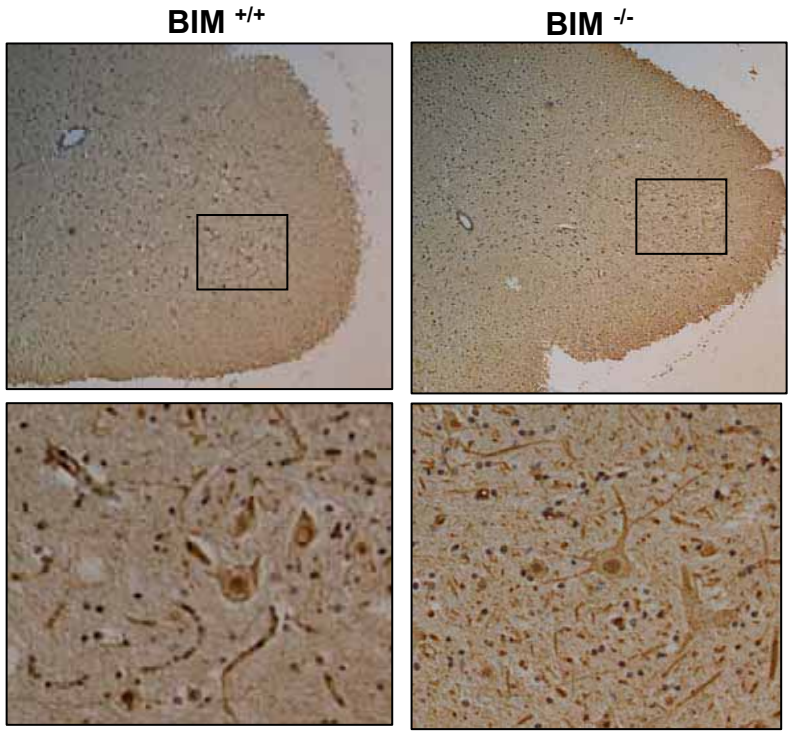
BIM +/+
BIM -/-

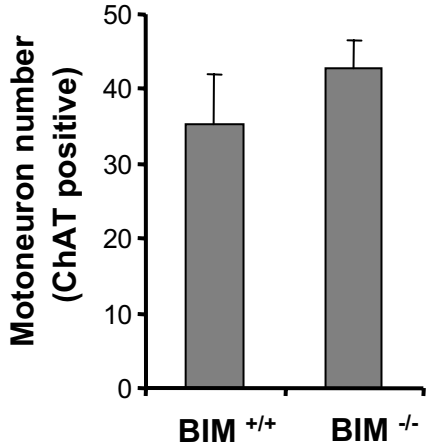
Motoneuron number
(ChAT positive)
50
40
30
20
10
0
BIM +/+
BIM -/-

Table 1. Real time PCR primers for BCL-2 related genes

Symbol	Organism	Forward	Reverse
Bad	Mouse	L745 cagccaccaacagtcatcat	R854 gctaagctcctcctccatcc
Bak	Mouse	L254 aatggcatctggacaaggac	R387 gttcctgctggtggaggtaa
Bax	Mouse	L357 gctgacatgtttgctgatgg	R467 gatcagctcgggcactttag
Bcl2	Mouse	L527 agtacctgaaccggcatctg	R657 gctgagcagggtcttcagag
Bclx	Mouse	L802 gctgggacacttttgtggat	R931 aagagtgagcccagcagaac
Bid	Mouse	L281 ctgcctgtgcaagcttactg	R424 atgtctggcaatgttgtgga
Bik	Mouse	L161 gagactcccagcatgaagga	R278 gcagacacaggtccatctca
Bim	Mouse	L619 cgacagtctcaggaggaacc	R733 catttgcaaacaccctcctt
Bmf	Mouse	L468 cccataagccaggaagacaa	R605 agggagaggaagcctgtagc
NOXA	Mouse	L270 ggagtgcaccggacataact	R388 ttgagcacactcgtccttca
PUMA	Mouse	L 537 gcccagcagcacttagagtc	R729 ggtgtcgatgctgctcttct